Modeling of Strong Ground Motion in "The Geysers" Geothermal Area

Nitin Sharma[1], Vincenzo Convertito[2], Nils Maercklin[3,1] and Aldo Zollo[1]

(1) Dipartimento di Scienze Fisiche, Università degli studi di Napoli "Federico II", RISSC-Lab, Napoli, Italy (2) INGV, Osservatorio Vesuviano, Napoli, Italy (3) AMRA Scarl Napoli, Italy

A360 EGU2012-2956

European Geosciences Union General Assembly 2012

Vienna | Austria | 22 – 27 April 2012

1. Introduction

Enhanced Geothermal Systems (EGSs) provide an increasingly important contribution to the world energy inventory. However, one of the controversial issues associated with EGSs is induced seismicity, which has been the cause of delays and threatened cancellation of at least two EGS projects worldwide (Majer *et al.*, 2007). Although induced seismicity may have light-to-moderate adverse physical effects on operations or on the surrounding communities, public concern about the rate and magnitude of the seismicity associated with current and future EGS operations still remain. The Geysers is the well-suited case study as it is world's largest geothermal field and has produced worthy data for seismologist since 1960.

Currently, there are no specific Ground Motion Prediction Equations (GMPEs) available for The Geysers field, although they play a key role in seismic hazard analysis and for monitoring the effects of the seismicity rate levels on inhabitants living in surrounding areas and on structures. The aim of the present study is the estimation of suitable GMPEs to be used at The Geysers geothermal area for monitoring purposes. In particular, the GMPEs are retrieved for PGV, PGA and Sa (T=1.0sec) as these ground-motion parameters are readily available after each earthquake, can be used to estimate potential damage and are well correlated with levels of human sensitivity (Bommer *et al.*, 2006). This issue is particularly important in all the applications devoted to real-time monitoring and seismic risk reduction in geothermal areas (Bommer *et al.*, 2006; Bachman *et al.*, 2011; Convertito *et al.*, 2011).

2. Data description

We retrieved data from the Northern California Earthquake Data Center (NCEDC) for an area around The Geysers (figure 1) and for the period 2007/09/01 through 2010/11/15. The data correspond to waveforms from 212 earthquakes recorded at 29 three-components stations of the Berkeley-Geysers (BG) network (red triangles in figure 1). The magnitude range of the events is 1.0 < Mw < 3.5, while a focal depth less than 5 km has been used for the analysis, because induced earthquakes are generally observed at shallow depths and the seismicity at larger depth is very low and ascribable to natural earthquakes. The hypocentral distance ranges between 0.5 km and 20 km.

2.1 Magnitude M_d Vs M_w

The size of largest portion of earthquakes are described by duration magnitude (M_d). However, in order to obtain results compatible with other studies and which could also be implemented for seismic hazard analysis purpose, we converted M_d into moment magnitudes M_w using a linear relationship :

$$M_w = a + bM_d \qquad (1)$$

The fit is shown in figure 2 and coefficients with uncertainty are shown in table 1.

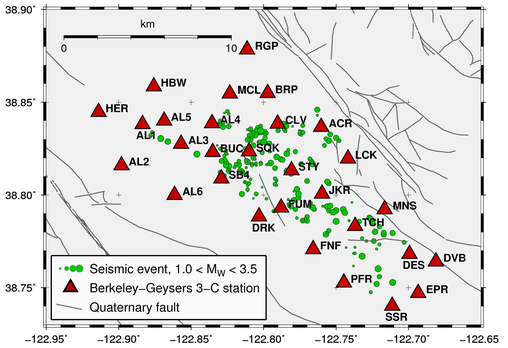

Figure 1 Location of events (green circles) and seismic stations (red triangles) used for regression analysis

2.2 Data preparation

We have analysed only high quality waveforms with signal to noise ratio larger than 10. The instrumental correction is applied in frequency band ranging between 1 Hz and 25 Hz to measure correct physical units.

Mean and trend are also removed. Further to measure appropriate PGA and PGV, we have cut the waveforms in a specific time window around the event starting at the origin time and ending at the time corresponding to 98% of total energy. Once the window is selected PGV is measured as largest value among horizontal components. The waveforms are then differentiated and filtered in band between 1Hz and 15Hz to measure PGA and the 5% damped spectral ordinate at 1 sec which as for PGV corresponds to largest among 2 horizontal components. Example is shown in figure 3.

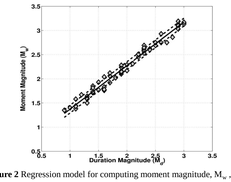

Figure 2 Regression model for computing moment magnitude, M_w , from duration magnitude M_d

Table 1: Regression coefficients and relative uncertainty for equation (1).

$a \pm \sigma_a$	$b \pm \sigma_b$	σ_{Total}	R^2
0.473±0.035	**0.900±0.017**	**0.080**	**0.980**

References

•Abrahamson, N.A., and R. R. Youngs (1992). A stable algorithm for regression analysis using the random effect model, *Bull. Seism. Soc. Am.* 82, 505-510.

•Abrahamson, N. A., and W. J. Silva (1997). Empirical Response Spectral Attenuation Relations for Shallow Crustal Earthquakes, *Seism. Res. Lett.* 68, 94-127.

•Bachmann, C. E., S. Wiemer, J. Woessner, and S. Hainzl (2011). Statistical analysis of the induced Basel 2006 earthquake sequence: introducing a probability-based monitoring approach for Enhanced Geothermal Systems, *Geophys. J. Int.*, 186(2), 793–807.

•Bommer, J.J., S.J. Oates, M. Cepeda, C. Lindholm, J. Bird, R. Torres, G. Marroquín, J. Rivas (2006). Control of hazard due to seismicity induced by a hot fractured rock geothermal project, *Eng. Geol.* 83, 287-306.

•Convertito, V., and A. Zollo (2011). Assessment of pre-crisis and syn-crisis seismic hazard at CampiFlegrei and Mt. Vesuvius volcanoes, Campania, southern Italy. *Bull. Volcanol.*, 73, 767–783.

•Emolo, A., V. Convertito , L. Cantore (2011). Ground-motion predictive equations for low-magnitude earthquakes in the campania-Luciana area, Southern Italy, *J. Geophy. Eng.*, 8, 46-60

•Majer, E.L., R. Baria, M. Stark, S. Oates, J. Bommer, B. Smith, and H. Asanuma (2007). Induced seismicity associated with Enhanced Geothermal Systems, *Geothermics.* 36, 185-222.

•McGarr, A. (1984). Scaling of ground motion parameters, stress, and focal depth. *J. Geophys. Res.* 89,6969-6979.

•Wald, D. J., V. Quitoriano, T. H. Heaton, H. Kanamori, C. W. Scrivner, and C.B. Worden (1999). TriNet ShakeMaps: Rapid generation of instrumental ground motion and intensity maps for earthquakes in southern California, *Earthq. Spectra.* 15, 537-555.

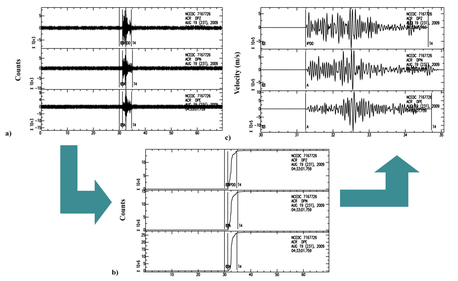

Figure 3 Example illustrating the procedure to cut the appropriate duration of waveforms for measuring peak-ground parameters (a) original traces, (b) energy computation to mark appropriate duration (c) the traces after cutting with instrumental correction as well.

Table 2: Regression coefficients and relative uncertainty of equation (2), using MOD1.

Values	$a \pm \sigma_a$	$b \pm \sigma_b$	$c \pm \sigma_c$	$h \pm \sigma_h$	$\sigma_{Inter\text{-}event}$	$\sigma_{Intra\text{-}event}$	σ_{Total}	R^2
PGV (m/s)	-4.977 ±0.075	1.325 ±0.022	-2.100 ±0.055	1.842 ±0.2108	0.159	0.343	0.379	0.814
PGA (m/s^2)	-3.135 ±0.080	1.271 ±0.021	-2.206 ±0.064	2.178 ±0.221	0.145	0.359	0.387	0.796
Sa(T=1.0s) (m/s^2)	-5.571 ±0.070	1.473 ±0.022	-1.549 ±0.049	1.411 ±0.287	0.158	0.358	0.391	0.814

Table 3: Regression coefficients and relative uncertainty of equation (3), using MOD2.

Values	$a \pm \sigma_a$	$b \pm \sigma_b$	$c \pm \sigma_c$	$h \pm \sigma_h$	$d \pm \sigma_d$	$\sigma_{Inter\text{-}event}$	$\sigma_{Intra\text{-}event}$	σ_{Total}	R^2
PGV (m/s)	-4.629 ±0.250	1.325 ±0.022	-2.687 ±0.384	2.363 ±0.359	0.025 ±0.015	0.159	0.343	0.379	0.814
PGA (m/s^2)	-2.853 ±0.289	1.271 ±0.021	-2.666 ±0.438	2.566 ±0.400	0.019 ±0.017	0.145	0.359	0.387	0.796
Sa(T=1.0s) (m/s^2)	-5.319 ±0.209	1.472 ±0.022	-2.002 ±0.331	1.968 ±0.449	0.021 ±0.014	0.158	0.358	0.391	0.814

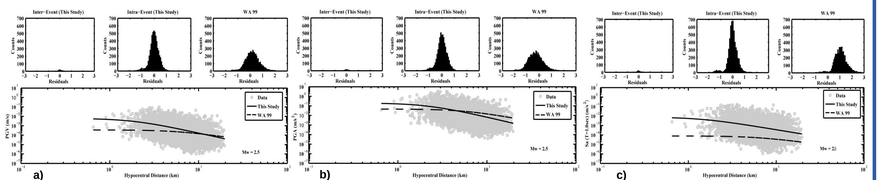

Figure 4 Fitting and comparison of the regression model MOD 1 with model proposed by Wald et al. (1999) panel (a) refers to PGV panel (b) refers to PGA and panel (c) refers to Sa(T=1.0 sec). Each panel shows the respective parameter as a function of distance and the residuals as histograms.

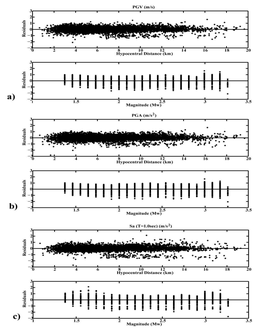

Figure 5 Distribution of residuals with respect to hypocentral distance and magnitude obtained from model MOD1, for PGV, PGA and Sa(T=1.0 sec).

3. Regression analysis

Non-linear Mixed effect regression analysis (NLRMA) is done to obtain GMPEs (Abrahamson and Youngs, 1992). This method has the advantage that it accounts for inter-event and intra-event effects. First a reference model is computed without explicit site/station corrections. To retrieve the final model, in a second regression, station corrections are introduced based on the mean residuals and Z-test results. We have tested two models which differ in terms of anelastic attenuation. The first model (MOD1) is expressed as:

$$\mathbf{Log_{10}Y = a + bM_w + cLog_{10}(\sqrt{(R_{hypo}{}^2 + h^2)})} \qquad (2)$$

Where Y is PGV in m/s , PGA and Sa (T=1.0sec) in m/s^2 and R_{hypo} is hypocentral distance in km and h is parameter used to avoid unrealistic high values at short distances. The coefficients of MOD1 are listed in table 2. The second model (MOD2) which considers the anelastic attenuation, is expressed as :

$$\mathbf{Log_{10}Y = a + bM_w + cLog_{10}(\sqrt{(R_{hypo}{}^2 + h^2)}) + dR_{hypo}} \qquad (3)$$

but it does not improve the model (see Table 3) hence we choose MOD1 which is expressed by less number of parameters. MOD1 is also compared with the model proposed by Wald et al. (1999) (WA 99) which is implemented in ShakeMap® shown in figure 4. PGV and PGA are showing good matching but for Sa (T=1.0sec) predictions are underestimated. (see figure 5).The distribution of residuals as function of distance and magnitude for entire data set is also studied, but no correlation is observed (see figure 6).

4. Station correction and corrected model

After obtaining the reference model we applied the same approach adopted by Emolo et al. (2011) to introduce a first order site/station effect correction. To this aim, we analysed the residual distribution at each station obtained by using the reference model MOD1.Then through Z-test, we tested the null hypothesis of a Gaussian Zero-mean distribution at 95% level of confidence. We assume that a deviation from the expected zero-mean value can be ascribed to a site/station effect which can be corrected. Station effect introduced here should be considered in a broad way as compared with the classical definition which accounts for soil condition just below the recording station. Based on the result of the Z-test, in terms of both value and sign, at each station we assigned dummy variable ***s*** whose value is -1,0 or +1.The retrieved ***corrected model (MOD3)*** is formulated as:

$$\mathbf{Log_{10}Y = a + bM_w + cLog_{10}(\sqrt{(R_{hypo}{}^2 + h^2)}) + es} \qquad (4)$$

The inferred coefficients together with their uncertainties are listed in table 4. It should be noted that total standard error has reduced in MOD3 and the residual are more centred at zero as compare to MOD1 as shown in figure 6. Fitting of MOD3 is shown in figure 7.

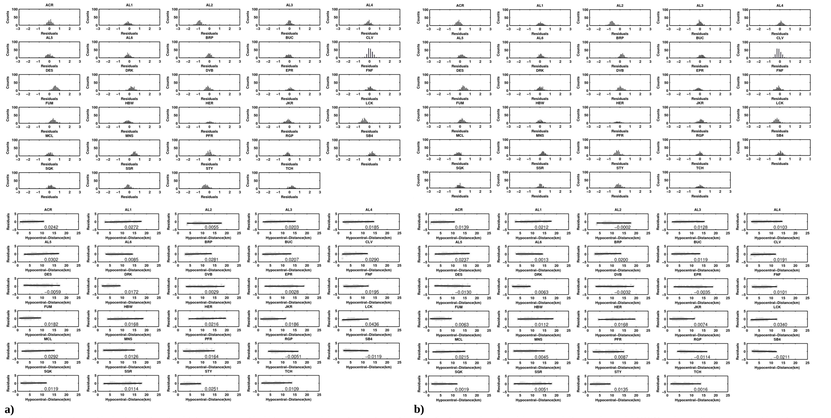

Figure 6 Single station residuals distribution. Panel (a) up, shows residual histograms and down is showing residual distribution as a function of hypocentral distance for model MOD1 and panel (b) up, shows residual histograms and down is showing residual distribution as a function of hypocentral distance for model MOD 3 , at each station for PGA only.

Table 4: Regression coefficients and relative uncertainty of equation (4), using MOD 3.

Values	$a \pm \sigma_a$	$b \pm \sigma_b$	$c \pm \sigma_c$	$h \pm \sigma_h$	$d \pm \sigma_d$	$\sigma_{Inter\text{-}event}$	$\sigma_{Intra\text{-}event}$	σ_{Total}	R^2
PGV (m/s)	-5.080 ±0.070	1.327 ±0.023	-1.965 ±0.047	1.866 ±0.190	0.189 ±0.004	0.169	0.288	0.334	0.857
PGA (m/s^2)	-3.245 ±0.073	1.273 ±0.021	-2.079 ±0.054	2.246 ±0.195	0.208 ±0.004	0.153	0.294	0.332	0.851
Sa(T=1.0s) (m/s^2)	-5.479 ± 0.074	1.473 ± 0.022	-1.664 ± 0.053	1.963 ±0.250	0.168 ± 0.004	0.164	0.316	0.356	0.846

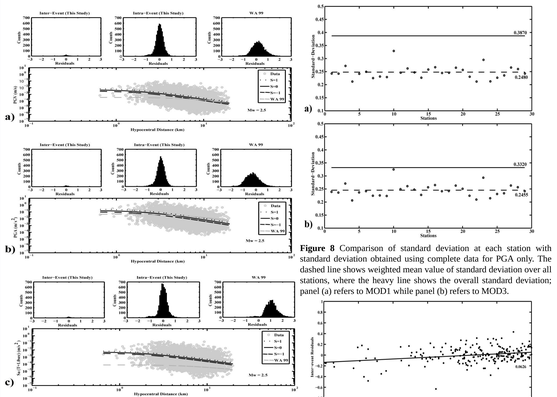

Figure 7 Fitting of MOD3 after the station correction . Panel (a) refers to PGV panel (b) refers to PGA (c) refers to Sa(T=1.0sec)

Figure 8 Comparison of standard deviation at each station with standard deviation obtained using complete data for PGA only. The dashed line shows weighted mean value of standard deviation over all stations, where the heavy line shows the overall standard deviation; panel (a) refers to MOD1 while panel (b) refers to MOD3.

Figure 9 Distribution of inter-event residuals obtained from PGA data with respect to event-depth by using MOD3, the positive trend sign.

Standard deviations at each station before and after site/station correction are analysed. The average of these station specific values for all the stations weighted by the number of observations per station, are shown in Figure 8 and are compared with the standard error of the regression obtained from the entire multi-station database (29 stations). The standard error at each station is lower than the total statndard error obtained from the entire multi-station database. Similar results are observed for PGV and Sa(T=1sec) but we are showing results for PGA only. The scatter among standard deviations has reduced by using MOD3 (figure 8b) as compared with MOD1 (figure 8a).

In addition, we have also analyzed the inter-event residual distribution using MOD3. As shown in Figure 9, for the analyzed data we have observed a slight positive trend of inter-event residuals w.r.t. event depth, which indicates that there is a possible increase in the stress drop with depth as reported by McGarr (1984). The results here are shown for PGA only, although same results are observed for PGV and Sa(T=1.0sec).

Conclusions

- Non-linear Mixed-effect Regression Analysis (NLMRA) allows to separate the contributions of the inter-event and intra-event error to the total standard error (e.g., Abrahamson and Silva, 1997).
- If information about local geology is not available, our approach of introducing site/station effect parameters has shown a significant improvement in the models as well.
- The two components of the standard error (i.e., inter-event and intra-event) are related to source effect and local site effects, respectively. The reduction in total standard error after introduction of site/station effect correction is actually associated to a reduction of the intra-event component.
- The inter-event residuals distribution shows a slight positive trend with depth, which indicates a possible increase in the stress drop with depth being the PGA correlated with it (McGarr, 1984).

Contact: sharma@na.infn.it